Coupled trace element and Hf-isotope measurements of Hadean through Paleoarchean zircons from the Singhbhum Craton indicate derivation from a long-lived, mantle-derived protocrust

Heather Kirkpatrick[1,2]*, Emily Stoll[1], and Nadja Drabon[1]
[1]Department of Earth and Planetary Science, Harvard University, Cambridge, Massachusetts, USA
[2]School of Geosciences, University of Louisiana, Lafayette, Louisiana, USA
** corresponding author, hmkucla@gmail.com*

This paper is currently being revised following the first round of reviews from EPSL. The paper will be resubmitted within the next two months.

Abstract

Due to the dearth of rock records during the Hadean, little is known about early crustal chemistry and geodynamics. Here, we present zircon trace and rare earth element and Lu-Hf measurements of zircons ~ 3.3 Ga to ~ 4.2 Ga from the Older Metamorphic Tonalitic Gneiss in the Singhbhum Craton to better understand geodynamic changes during the Hadean and Archean. We find decreasing, subchondritic zircon ε_{HfT} among zircons > 3.8 Ga and no indication of addition of new crustal material during the Hadean after initial formation of this protocrust. Trace and rare earth element analyses of > 3.8 Ga grains indicate derivation from a source heavily influenced by the enriched mantle with little evidence for flux melting, and no clear evidence for deep melting. At ~ 3.8 Ga, we observe an average ε_{HfT} increase indicating new additions of juvenile material. These zircons still show predominantly mantle-like trace elements, but with the appearance of some arc-like trace element zircon signatures and evidence for crustal thickening. This period of crustal reorganization speaks towards a shift in geodynamic regime characterized by the onset of communication between the mantle and the crust from which the zircons formed at this location. The presence of long-lived, mantle-derived protocrust in both India and South Africa appears to suggest the possibility of a stagnant lid, albeit more data is necessary to confirm this. The presence of a transition of ε_{HfT} data globally may point towards an important period of crustal reorganization 3.9 – 3.6 Ga ago.
Keywords: Hadean-Archean, zircon, Hf isotopes, trace element chemistry

Highlights:

- OMTG grains > 3.8 Ga: derive from source heavily influenced by an enriched mantle
- Grains >3.8 Ga: little evidence for arc melting
- Grains < 3.8 Ga: dominantly mantle-like trace elements
- Grains < 3.8 Ga: minor arc-like trace elements & some evidence for crustal thickening
- 3.9 – 3.6 Ga: important period of crustal reorganization locally
- 3.9 -3.6 Ga: Potentially also important period of global crustal reorganization

1.1 Introduction

Despite decades of work on understanding early Earth magmatic chemistry, large gaps in knowledge still exist about tectonics and crustal compositions in the Hadean and Eoarchean. Only detrital or xenocrystic zircons from rare metamorphosed igneous or sedimentary rocks collected in Archean cratons retain information about that time period (Harrison, 2020). However, these Hadean zircon studies largely focus on a single site, the Jack Hills metaconglomerate in Western Australia (Peck et al., 2001; Mojzsis et al., 2001; Harrison et al., 2005; Watson and Harrison, 2005; Trail et al., 2007; Blichert-Toft and Albarède, 2008; Bell and Harrison, 2013; Bell et al., 2014, 2015, 2016, 2017; Borisova et al., 2022; Carley et al., 2022), resulting in a heavily biased geochemical record: To date, >10,000 Hadean detrital zircons have been found in the Jack Hills while only 50 have been discovered outside of the Jack Hills (Harrison, 2020). Regardless, studies of these sites, including extensive U-Pb and Pb-Pb dating to quantify rates of crustal production and preservation (Holden et al., 2009; Chaudhuri et al., 2018; Miller et al., 2018; Chaudhuri, 2020; Drabon et al., 2021), Lu-Hf to understand crustal evolution (Blichert-Toft and Albarède, 2008; Harrison et al., 2008; Kemp et al., 2010; Bell et al., 2014; Chaudhuri et al., 2018; Bauer et al., 2020a; Drabon et al., 2022), and trace and rare earth elements (TREE) to decipher crustal composition (Hoskin, 2005; Trail et al., 2007, 2011, 2017; Bell et al., 2016; Reimink et al., 2020; Turner et al., 2020; Ackerson et al., 2021; Borisova et al., 2022; Drabon et al., 2022; Carley et al., 2022), have allowed for unparalleled insights into early Earth.

One of the most pressing issues in Precambrian geology is the onset of plate tectonics – both in terms of the mechanism and timing. Previous studies found Hadean zircons display mostly subchondritic Lu-Hf with decreasing ε_{HfT} values through time (Blichert-Toft and Albarède, 2008; Kemp et al., 2010; Bell et al., 2014; Chaudhuri et al., 2018; Miller et al., 2018; Bauer et al., 2020b; Drabon et al., 2021), which are often interpreted to indicate reworking of a long-lived mafic protocrust, possibly in a stagnant lid environment (Bauer et al., 2020b; Ranjan et al., 2020). However, other studies interpret Lu-Hf results as continental in nature, possibly in a plate boundary setting (Harrison et al., 2008; Bell et al., 2014). For the Older Metamorphic Tonalitic Gneiss (OMTG), previous work has relied on very limited Hf isotopes. The only study directly exploring the initial $^{176}Lu/^{177}Hf$ of the source of the Hadean xenocrystic zircons is Chaudhuri et al. (2018). Using Lu-Hf analyses of three Hadean xenocrystic OMTG zircons, Chaudhuri et al. (2018) argued for extraction of crust from the mantle at 4.5 Ga and subsequent intracrustal reworking. They then used a trendline through these three analyses to argue for a mafic precursor crust that was remelted to form minor felsic magmas from which the zircons formed. Miller et al. (2018) reported one Lu-Hf value from a 4.015 ± 9 Ma zircon from modern river sand (ε_{HfT}= -5.30) which they argue provides support for a Hadean felsic crust, although the spatial and temporal extent of this remains ambiguous. Both the limited Lu-Hf data and the contrasting assertions about the OMTG Hadean xenocrystic zircon make Lu-Hf of additional Hadean grains at this site an important research direction.

Since there are multiple interpretations of Lu-Hf data, TREE may provide an additional avenue to differentiate between different origins of the long-lived Hadean crust, as they directly reflect separate aspects of melt composition. Previous work used zircon TREE to argue for a mantle-derived crustal origin of Hadean zircon in the Jack Hills (Borisova et al., 2022) and South Africa (Drabon et al., 2021, 2022) while others used it to argue for a continental origin (Carley et al., 2022). This discrepancy may be due to little high-quality in-situ Sc and Nb concentration data of Archean and Hadean zircon (Drabon et al., 2022, 2024; Mixon et al., 2024). Regardless, TREEs from those two locations alone are not sufficient to determine the global geodynamic regime. To further constrain what is possible for Hadean crustal generation worldwide, we need more locations analyzed for coupled Lu-Hf isotopes and TREE. Clearly, ambiguous results and a low number of locations calls for more research in other locations.

Further, while whole rock chemistry of the Singhbhum Craton has provided important information on the growth of the Singhbhum Craton, the oldest rocks in this region generally have emplacement ages <3.5 Ga (Dey et al., 2017; Olierook et al., 2019). For this reason, zircon > ~3.53 Ga provides an important perspective on the crustal evolution in the Singhbhum Craton before the oldest preserved rocks.

Here, we present U-Pb, TREE, and Lu-Hf data from a suite of zircons from the Older Metamorphic Tonalitic Gneiss (OMTG) in the Singhbhum Craton of eastern India to infer the composition of the early crust from which the zircons were derived and make inferences for possible changes in geodynamic regime.

1.2 Geologic Background

The Paleoarchean Singhbhum Craton is located in northeastern India (Mukhopadhyay, 2001) (Figure 1A, B). The two oldest units are part of the Older Metamorphic Group, which is composed of metasedimentary rocks and amphibolites, and the OMTG. The latter represents TTGs (tonalite–trondhjemite–granodiorite) that formed over four stages between from 3.53 and 3.32 Ga and contains the oldest zircons found in the Singhbhum Craton (Dey et al., 2017; Chaudhuri et al., 2018; Olierook et al., 2019; Chaudhuri, 2020) (Figure 1A). Between 3.30 and 3.28 Ga, and after the formation of the OMTG, extensive amphibolite to greenschist facies-grade metamorphism occurred (Upadhyay et al., 2014). Whole rock chemistry among a subset of TTG samples indicates variably low HREE contents and high Sr/Y (e.g. Chaudhuri, 2020), indicating some formation at high, garnet-bearing pressures (Dey et al., 2019). However, since there is a large amount of inherited zircon in these TTGs, connecting whole rock chemistry to specific dates can be difficult and imprecise.

Previous studies of the OMTG report xenocrystic zircons > 4.0 Ga (Chaudhuri et al., 2018; Miller et al., 2018) with age peaks through the Paleoarchean at 3.61 and 3.46-3.41 Ga (Upadhyay et al., 2014). OMTG zircons < 3.8 Ga are close to ε_{HfT} = 0, with values extending down to ε_{HfT} = ~ -8, indicating both reworking of older crust and juvenile additions. Other studies of adjacent Archean igneous rocks (Chaudhuri et al., 2018) and river sediment (Miller et al., 2018) have average ε_{HfT} which are, in general, more positive (ε_{HfT} = ~ -10 to ~ +10; Figure 2) and which can be interpreted to indicate substantial addition from a potentially more depleted source (Chaudhuri et al., 2018; Miller et al., 2018; Mitra et al., 2019). Importantly, sparse data has been published for OMTG zircon ~3.4 Ga to ~3.7 Ga (7 grains within 10% of concordia) and the Hadean (6 dated grains with 3 ε_{HfT} points).

2 Methods

~ 3000 OMTG zircon, along with several standards including FC-1 (Paces and Miller, 1993; Schmitz et al., 2003), R33 (Black et al., 2004), MAD-559 (Coble et al., 2018), and OG1 (Bodorkos et al., 2009), were separated and mounted to make epoxy pucks. U-Pb and Lu-Hf measurements were performed at Arizona LaserChron Center (Cecil et al., 2011; Gehrels and Pecha, 2014), and trace and rare earth elements in addition to U-Pb measurements for a subset of grains, were performed at the Stanford-USGS SHRIMP-RG lab (Premo et al., 2010). See information on the sample collection and processing, as well as data collection and reduction in the supplementary material.

2.1. Sample collection, processing and analysis

Sample OMTG was collected from the same location as the rock presented in Chaudhuri et al. (2018) (22.61044°N, 86.21775°E), and sample processing occurred at Harvard University and followed standard procedures (Drabon et al., 2019)), supplementary text).

After polishing, a series of U-Pb runs were performed using the E2 and Nu2 LA-ICPMS instruments at the Arizona LaserChron Lab from 2021-2023 (Gehrels et al., 2008). Results were standardized to FC1 (Paces and Miller, 1993; Schmitz et al., 2003) and R33 (Black et al., 2004) using the data reduction software AgeCalc_ML (Sundell et al., 2020), and OG1 ages were compared to published standard ages to ensure correct data reduction (Bodorkos et al., 2009). 429 Pb-Pb LA-ICP-MS dates passed selection criteria and were within 10% of concordia (Table S1). A subset of grains were dated via U-Pb analysis at the Stanford University-USGS SHRIMP facility (Table S2) (Premo et al., 2010). There is good agreement between ICP-MS and SHRIMP-RG ages.

Trace and rare earth concentration measurements (TREE) were performed at the Stanford University-USGS SHRIMP facility during two sessions in 2021 and 2023 following the same procedures as Drabon et al. (2022). Measurements were standardized to MAD-559 (Coble et al., 2018). All data, including those which failed our rejection criteria, are in Tables S3, S4, and S5. Of those that passed, 15 analyses represent 14 zircons >3.8 Ga.

Hf isotopes were performed at ALC using the Nu2 in August 2023 (Gehrels and Pecha, 2014; Ibañez-Mejia et al., 2014). Zircons with oscillatory zoning were targeted and measurements were made either on top of the Pb-Pb pit or, in the case of grains with alteration, within the same zone (Figure S1). In all, 25 samples have correlated U-Pb, TREE, and Lu-Hf analyses.

2.2 Assessing alteration affecting Hf isotope and trace element compositions

Results from measurements on metamict or strongly altered areas of zircon can lead to erroneous results. As such, we took several steps to reduce incorporation of these results including through screening of data by cathodoluminescence, backscatter electron, and transmitted light imaging of samples, cycle-by-cycle investigation of some measurements, and trace element chemistry.

CL zoning is a common proxy for radiation damage in zircon and concentrations of various heavy rare earth elements (REE) (Rubatto, 2017). Homogenous zoning is often argued to be a result of hydrothermal alteration, subsolidus formation, or formation from anatectic melts (Corfu et al., 2003; Rubatto, 2017). Our data reduction protocol removed analyses where multiple zones were analyzed (for example, SBC-OMTG Run 2 Spot 307) or where inclusions are obvious, but we generally kept analyses with homogenous CL zoning. Many OMTG Hadean zircon do not exhibit oscillatory zoning, which required us to also target grains with homogenous zoning. However, we do not find a difference in Lu-Hf results among zircons with homogenous or oscillatory zoning, suggesting minimal Hf mobility (Lenting et al., 2010) (Figure S4A). We also note that previous studies (Chaudhuri et al., 2018; Miller et al., 2018) did not remove points based on CL zoning. Imaging of pits was performed after analyses using an optical microscope. Measurements performed on areas of alteration or inclusions were removed.

TREE data were filtered using indicators suggested by Grimes et al. (Grimes et al., 2015) and include removing grains with high Al (>1000 ppm), Ca (>50 ppm), or P (>1000 ppm), or large (>50 Ma) error bars (2σ). Analyses performed on large cracks were also removed. In total, we performed 157 analyses with 68 passing our filters.

Coupled trace element and Lu-Hf analyses were taken where possible on a subset of grains, with the trace element analyses performed before the Lu-Hf analyses. We do not observe a substantial difference between Hf measurements on grains where analyses passed the TREE filters, failed the TREE filters, or where TREE measurements were not performed (Figure S4B), which provides reassurance of the limited mobility of Hf in these zircons. However, although we were conservative with which points passed our selection criteria, alteration may have impacted some grains. For this reason, we look at trends in εHf rather than individual points. To allow the reader to directly assess potential alteration, cathodoluminescence images of a subset of grains are shown in Figure S1.

3. RESULTS

Zircon ages range between 4185 ± 10 Ma (2σ) (SHRIMP U-Pb age; Table S2) and 3060 ± 21 Ma (2σ) (LA-ICPMS U-Pb age; Table S1). 17 zircons are older than 3.8 Ga (Figure 3; Table S1) and we observe a small age peak between 4.0 and 4.1 Ga. Few zircons are present between ~3.7 and ~4.0 Ga (Figure 3). A peak at ~3.4 Ga is non-Gaussian with subpeaks at ~3.47 and ~3.58 Ga. Previous studies estimated the date of emplacement for the TTG component of the OMTG to be 3530 to 3300 Ma (Nelson et al., 2014), which our results support. Many of the grains are complex with CL evidence for multiple growth episodes and areas of recrystallization, while others show only faint oscillatory or homogenous zooming (Figure S1). All filtered data have Th/U ratios > 0.1, in agreement with a primary igneous origin (Figure 4A) (Rubatto, 2017).

Zircon TREE shows evidence for at least two large geochemical shifts occurring at 3.8 Ga 5and 3.45 Ga (2-sample t-test, supplemental material). Among zircon >3.8 Ga, Sc/Yb (median: 0.030) and U/Nb data (median: 11.5) plot within the mantle field (Figure 5; Tables S3, S4, and S5). Eu/Eu* values, which may relate to changes in plagioclase stability, redox, or presence of water, show relatively low values until 3.8 Ga (median: 0.21) (Trail et al., 2011, 2012; Burnham and Berry, 2012; Loucks et al., 2020; Tang et al., 2020). Ce/Nd values are also relatively low (median: 2.48), possibly indicating a relatively reduced signature compared to younger zircons. Both zircon Sc/Yb and U/Yb gradually increase throughout the Hadean (Figure 4B, C). At ~3.8 Ga, Sc/Yb increases (median: 0.091) and Nb/Yb decreases (median: 0.030) (Figure 4B, D). While most data still plot within the mantle field, a subset of grains fall within the arc-like melting field when considering Sc/Yb vs. Nb/Yb, and U/Nb vs. time (Figs. 4B and 3D). This change coincides with increasing values of Eu/Eu* (median of 0.31), while Ce/Nd values stay about the same (median: 2.61). The second large shift at ~3.45 Ga is primarily seen in redox-sensitive TREE proxies with a sharp increase in both Ce/Nd (median: 5.88) and Eu/Eu* (median: 0.37) (Fig. 3F, G). Additionally, we observe a shift to higher Th/U at 3.45 Ga (>3.8 Th/U = 0.56; 3.45-3.8 Ga Th/U = 0.57; <3.45 Ga Th/U = 0.86). Additional figures are included in the supplement. Most of these changes are statistically significant based on a series of 2-sample t-tests, which assumed unequal variances ($p < 0.05$; and Table S6). Vertical lines on Figure 4 note these statistically significant transitions.

Hf isotopes reveal zircons > 3.8 Ga have subchondritic ε_{HfT} values and form an approximate linear array with a negative slope ($^{176}Lu/^{177}Hf$ ~ -0.010) from -2 to -8 ε_{HfT} units (Table S7; Figure 2) when the array intersects CHUR at ~4.4 Ga. Most zircons < 3.8 Ga have values near or above $\varepsilon_{HfT} = 0$, with most values ranging between +7 and -3 units indicating the introduction of juvenile material, with only three exceptions. These three exceptions plot more substantially below CHUR, along the crustal evolution array of the Hadean protocrust, and may reflect the last preserved isotopic remanence of this long-lived crust. These Hf isotope results are similar to previous studies (Dey et al., 2017; Chaudhuri et al., 2018; Miller et al., 2019; Pandey et al., 2019; Sreenivas et al., 2019; Ranjan et al., 2020; Gond et al., 2023).

4. DISCUSSION

4.1 Crustal evolution as recorded in the OMTG

Decreasing, subchondritic zircon ε_{HfT} among zircons > 3.8 Ga indicate extraction of Hadean protocrust sometime between 4.5 to 4.3 Ga followed by internal reworking of this crust over >500 million years (Figure 2). Importantly, our ε_{HfT} results indicate no addition of new crustal material during the Hadean after initial formation of a protocrust. Previously, Chaudhuri et al. (2018) determined the slope of the $^{176}Lu/^{177}Hf$ line from three datapoints ($^{176}Lu/^{177}Hf$ = 0.019), which they used to argue for xenocrystic zircons from the OMTG being derived from mafic crust and a CHUR extraction age of 4.497 ± 0.19 Ga. Our results show a far more ambiguous picture with results that do not provide a definitive extraction age or $^{176}Lu/^{177}Hf$ slope. Depending on whether we assume extraction 4.5 Ga or 4.3 Ga, our data best fit with a felsic source ($^{176}Lu/^{177}Hf$ = ~0.006; 4.3 Ga; n=11) or a quite mafic source ($^{176}Lu/^{177}Hf$ = 0.020; 4.5 Ga, n= 11). Additionally, we note that $^{176}Lu/^{177}Hf$ is approximately the same whether we use only new data or new data and OMTG data published in Chaudhuri et al. (2018) for each extraction age. This clearly shows that unless grains truly form a linear array and there are enough grains to form a significantly significant sample size, it is very challenging to determine both the time of extraction and the $^{176}Lu/^{177}Hf$ of the source (and thus the relative composition). We include $^{176}Lu/^{177}Hf$ values which range from mafic (0.0193) to relatively more felsic (0.0115) and time of extraction at 4.5 Ga and 4.3 Ga to visualize potential trajectories of ε_{HfT} (Figure 2).

While our new and previous ε_{HfT} data remain ambiguous as to the nature of the isolated crust, TREE can help determine the origin of the crust. Low Sc/Yb and U/Nb together with elevated Nb/Yb suggest an origin of this protocrust from an undepleted mantle (Figure 5B), indicating a non-hydrous, and likely non-arc-like, melting source for most sampled zircon (Figure 5B). Proxies for melting depth show no evidence for particularly deep melting, such as seen in Iceland. For melting depth estimates, the opposite stability of plagioclase (shallow crust) and garnet (deep crust) are commonly used. The Eu/Eu* anomaly suggests the presence of plagioclase at relatively shallow crustal depth and/or a more reduced system, and Dy/Yb is within range of typical shallow fractionation in the absence of garnet (Claiborne et al., 2010) unless amphibole was abundantly present (Fig. S2). Together, this points to an initial extraction of long-lived crust from the mantle in the Hadean followed by anhydrous remelting at a relatively shallow depth.

A change in ε_{HfT} values and TREE suggests a dramatic shift in geodynamic regime at ~3.8 Ga. The increase in average ε_{HfT} indicates a transition towards more frequent mantle additions (Figure 2), supporting previous work by (Chaudhuri et al., 2018). In addition, median Sc/Yb increases, with some grains exhibiting arc-like Sc/Yb, while a strong mantle signature persists in many grains (Figs. 3B and 4B). Arc-like Sc/Yb is typically interpreted to be heavily influenced by fluid-assisted melting and/or a starting melt with higher Zr, allowing for less differentiation before zircon saturation (Boehnke et al., 2013; Grimes et al., 2015). With this change, we see an increase in Eu/Eu* (Figure 5F). We interpret the increase in Eu/Eu* after 3.8 Ga to indicate formation from a deeper source due to the lack of co-variation with Ce/Nd that would support a change in oxygen fugacity (Figure 5G). With increased pressures, plagioclase breakdown and garnet stability results in an increase of redox-sensitive TREE in zircon, including Eu/Eu* (Tang et al., 2020). Together, these zircons show abundant juvenile additions with dominantly mantle signatures and some, but limited, evidence for hydrous melting. This could represent a thick oceanic plateau with episodic hydrous melting events, in agreement with geological observations from the Singhbhum Craton (Dey et al., 2017, 2019; Chaudhuri et al., 2018; Mitra et al., 2019; Olierook et al., 2019; Chaudhuri, 2020). This strong mantle signature contrasts to other similarly aged zircons in other Paleoarchean sequences such as those in the Barberton Greenstone Belt (South Africa), which show abundant evidence for hydrous melting ((Drabon et al., 2021; Drabon et al., 2022; Drabon et al., 2024).

After 3.45 Ga, a coupled increase in both Eu/Eu* and Ce/Nd suggests more oxidizing conditions. A more oxidating environment is also supported by the increase in Th/U (Burnham and Berry, 2012). The coincidence of this shift and a previously suggested large-scale crustal extraction at ~3.45 (Upadhyay et al., 2019, Pandey et al. 2019) potentially points to early hydrous melting. Previous studies found 3.44-3.45 Ga TTGs in the region are depleted in heavy REE and are likely derived from a rutile-free and garnet and amphibole-bearing source that was at 10-15 kbar (Upadhyay et al., 2019). Additionally, Upadhyay et al. (2019) found through Hf and Nd isotope analysis of 3.44-3.45 granitoids that these rocks have both juvenile and Eoarchean signatures, which supports our assertion of large-scale extraction at ~3.45 Ga (Upadhyay et al., 2019).

In summary, the evolution of the crust as reflected in the OMTG zircons reveals a three-stage evolution, from (1) Long-lived protocrust apparently isolated from the mantle as no new mantle additions are recorded, (2) crustal thickening and new mantle additions, reflecting the onset of exchange between the crust and mantle starting at 3.8 Ga, to (3) a shift to more oxidizing conditions at 3.45 Ga.

4.2 Global comparison

While each Eoarchean to Hadean zircon suite is going to necessarily reflect local changes in the crustal evolution, it may indicate a global transition if a similar shift is traceable in other zircon suites around the Earth. There appears to be a shift in crust production between ~3.9 Ga and ~3.6 Ga based on a global shift in zircon ε_{HfT} (Bell and Harrison, 2013; Bell et al., 2014; Griffin et al., 2014; Frost et al., 2017; Bauer et al., 2020b; Drabon et al., 2022) and, at least where measured in the Jack Hills, Barberton Greenstone Belt, and Singhbhum Craton, trace element chemistry (Bell et al., 2014; Ranjan et al., 2020; Drabon et al., 2022; Carley et al., 2022) (Figure 6). This may provide evidence for a diachronous global shift in geodynamics, although more data is necessary to confirm this. What is remarkable is the longevity of the >3.9 Ga crust in all ancient zircon suites with initial extraction from the mantle and continued intracrustal reworking for hundreds of millions of years. As early as ~3.9 Ga, although the shift in some regions commences as late as 3.6 Ga, crust production shifted to an environment with more dynamic exchange between the mantle and evolved crust. This is indicated by frequent new mantle additions, and the more common appearance of flux melting.

For at least two locations, the Singhbhum Craton (this study) and the Barberton Greenstone Belt (Drabon et al., 2021, 2022), this Hadean long-lived crust was derived from the enriched mantle and shows little evidence for arc-like melting processes. Hence, after initial extraction from the mantle the crust was continuously internally reworked with little evidence for subduction. The absence of crust and mantle interaction and the longevity of the mantle-derived crust stands in contrast to modern style plate tectonics, where new mantle-derived crust formed in MOR is destroyed within 200 Ma. This may provide evidence for a stagnant lid.

At the same time, the trace element geochemistry of zircons that formed other locations similarly interpreted to have been long-lived protocrust show a variety of signatures. Many zircons from the Jack Hills and Acasta Gneiss complex appear to have been derived from fluxed melting processes (Harrison, 2020; Turner et al., 2020; Borisova et al., 2022; Carley et al., 2022; Mixon et al., 2024) albeit high-precision measurements of Sc and Nb are still rare. At this point, more data is necessary to more firmly assess the diversity of crustal rocks produced during the Hadean and the possibility of (episodic) crustal mobility, transient local subduction without global plate tectonics, and/or the possibility of arc-like flux melting signatures caused by non-arc processes such as partial convective overturn. With a growing number of studies exploring a larger variety of ancient zircon sites, the view of an early Earth that contained diverse geochemistry and, likely, geodynamics, shows a lively planet where some level of crustal diversification had begun.

5 CONCLUSIONS

Our data indicates that the source of our > 3.8 Ga zircons was extracted from a fertile mantle source and remained in isolation for 500+ million years. Throughout this period of intracrustal reworking, this crust remained relatively thin. The geochemistry of >3.8 Ga zircons from the OMTG closely resembles that of other Hadean zircons from South Africa, which indicates drier melt conditions compared to >3.8 Ga zircons from the Jack Hills and Acasta Gneiss Complex. After a globally observed chemical and geodynamic change starting by 3.9 Ga (Aarons et al., 2020; Bauer et al., 2020a; Drabon et al., 2022; Carley et al., 2022), OMTG zircon, while still indicating a heavily mantle-derived source, show evidence for a shift to thicker crust which contain more arc-like or hydrous melting signatures.

6. ACKNOWLEDGMENTS

Funding was provided by NSF-EAR 2204595 (H.M.K.) and the Harvard University Department of Earth and Planetary Sciences (N.D.). We thank the staff at Arizona LaserChron Center, supported by NSF-EAR 2050246, and Stanford SHRIMP-RG Lab for assistance with analysis.

7. REFERENCES CITED

Aarons S. M., Reimink J. R., Greber N. D., Heard A. W., Zhang Z. and Dauphas N. (2020) Titanium isotopes constrain a magmatic transition at the Hadean-Archean boundary in the Acasta Gneiss Complex. *Science Advances* **6**, 1–9.

Ackerson M. R., Trail D. and Buettner J. (2021) Emergence of peraluminous crustal magmas and implications for the early Earth. *Geochemical Perspectives Letters* **17**, 50–54.

Bauer A. M., Reimink J. R., Chacko T., Foley B. J., Shirey S. B. and Pearson D. G. (2020a) Hafnium isotopes in zircons document the gradual onset of mobile-lid tectonics. *Geochemical Perspectives Letters* **14**, 1–6.

Bauer A. M., Vervoort J. D. and Fisher C. M. (2020b) Unraveling the complexity of zircons from the 4.0–2.9 Ga Acasta Gneiss Complex. *Geochimica et Cosmochimica Acta* **283**, 85–102.

Bell E. A., Boehnke P. and Harrison T. M. (2016) Recovering the primary geochemistry of Jack Hills zircons through quantitative estimates of chemical alteration. *Geochimica et Cosmochimica Acta* **191**, 187–202.

Bell E. A., Boehnke P., Harrison T. M. and Mao W. L. (2015) Potentially biogenic carbon preserved in a 4.1 billion-year-old zircon. *Proc Natl Acad Sci U S A* **112**, 1–4.

Bell E. A., Boehnke P. and Mark Harrison T. (2017) Applications of biotite inclusion composition to zircon provenance determination. *Earth and Planetary Science Letters* **473**, 237–246.

Bell E. A. and Harrison T. M. (2013) Post-Hadean transitions in Jack Hills zircon provenance: A signal of the Late Heavy Bombardment? *Earth and Planetary Science Letters* **364**, 1–11.

Bell E. A., Harrison T. M., Kohl I. E. and Young E. D. (2014) Eoarchean crustal evolution of the Jack Hills zircon source and loss of Hadean crust. *Geochimica et Cosmochimica Acta* **146**, 27–42.

Black L. P., Kamo S. L., Allen C. M., Davis D. W., Aleinikoff J. N., Valley J. W., Mundil R., Campbell I. H., Korsch R. J., Williams I. S. and Foudoulis C. (2004) Improved 206Pb/238U microprobe geochronology by the monitoring of a trace-element-related matrix effect; SHRIMP, ID–TIMS, ELA–ICP–MS and oxygen isotope documentation for a series of zircon standards. *Chemical Geology* **205**, 115–140.

Blichert-Toft J. and Albarède F. (2008) Hafnium isotopes in Jack Hills zircons and the formation of the Hadean crust. *Earth and Planetary Science Letters* **265**, 686–702.

Bodorkos S., Stern R., Kamo S., Corfu F. and Hickman A. (2009) OG1: A Natural Reference Material for Quantifying SIMS Instrumental Mass Fractionation of Pb Isotopes During Zircon Dating. *AGU Fall Meeting*.

Boehnke P., Watson E. B., Trail D., Harrison T. M. and Schmitt A. K. (2013) Zircon saturation re-revisited. *Chemical Geology* **351**, 324–334.

Borisova A. Y., Nédélec A., Zagrtdenov N. R., Toplis M. J., Bohrson W. A., Safonov O. G., Bindeman I. N., Melnik O. E., Pokrovski G. S., Ceuleneer G., Jochum K. P., Stoll B., Weis U., Bychkov A. Y. and Gurenko A. A. (2022) Hadean zircon formed due to hydrated ultramafic protocrust melting. *Geology* **50**, 300–304.

Burnham A. D. and Berry A. J. (2012) An experimental study of trace element partitioning between zircon and melt as a function of oxygen fugacity. *Geochimica et Cosmochimica Acta* **95**, 196–212.

Carley T. L., Bell E. A., Miller C. F., Claiborne L. L., Hunt A., Kirkpatrick H. M. and Harrison T. M. (2022) Zircon-modeled melts shed light on the formation of Earth's crust from the Hadean to the Archean. *Geology* **50**, 1028–1032.

Cecil M. R., Gehrels G., Ducea M. N. and Patchett P. J. (2011) U-Pb-Hf characterization of the central Coast Mountains batholith: Implications for petrogenesis and crustal architecture. *Lithosphere* **3**, 247–260.

Chaudhuri T. (2020) A review of Hadean to Neoarchean crust generation in the Singhbhum Craton, India and possible connection with Pilbara Craton, Australia: The geochronological perspective. *Earth-Science Reviews* **202**, 1–25.

Chaudhuri T., Wan Y., Mazumder R., Ma M. and Liu D. (2018) Evidence of Enriched, Hadean Mantle Reservoir from 4.2-4.0 Ga zircon xenocrysts from Paleoarchean TTGs of the Singhbhum Craton, Eastern India. *Scientific Reports* **8**, 1–12.

Claiborne L. L., Miller C. F. and Wooden J. L. (2010) Trace element composition of igneous zircon: temporal, thermal, and compositional record of magmatic processes in the Spirit Mountain Batholith, Nevada. *Contrib Miner Petrol* **160**, 511–531.

Coble M. A., Vazquez J. A., Barth A. P., Wooden J., Burns D., Kylander-Clark A., Jackson S. and Vennari C. E. (2018) Trace Element Characterisation of MAD-559 Zircon Reference Material for Ion Microprobe Analysis. *Geostandards and Geoanalytical Research* **42**, 481–497.

Corfu F., Hanchar J. M., Hoskin P. W. O. and Kinny P. (2003) Atlas of zircon textures. *Reviews in Mineralogy and Geochemistry* **53**.
Dey S., Mitra A., Nandy J., Mondal S., Topno A., Liu Y. and Zong K. (2019) *Early Crustal Evolution as Recorded in the Granitoids of the Singhbhum and Western Dharwar Cratons*., Elsevier B.V.
Dey S., Topno A., Liu Y. and Zong K. (2017) Generation and evolution of Palaeoarchaean continental crust in the central part of the Singhbhum craton, eastern India. *Precambrian Research* **298**, 268–291.
Drabon N., Byerly B. L., Byerly G. R., Wooden J. L., Keller C. B., Lowe D. R., Brenhin Keller C. and Lowe D. R. (2021) Heterogeneous Hadean crust with ambient mantle affinity recorded in detrital zircons of the Green Sandstone Bed, South Africa. *Proceedings of the National Academy of Sciences of the United States of America* **118**, 1–9.
Drabon N., Byerly B. L., Byerly G. R., Wooden J. L., Wiedenbeck M., Valley J. W., Kitajima K., Bauer A. M. and Lowe D. R. (2022) Destabilization of Long-Lived Hadean Protocrust and the Onset of Pervasive Hydrous Melting. *AGU Advances* **e2021AV000**, 1–17.
Drabon N., Galić A., Mason P. R. D. and Lowe D. R. (2019) Provenance and tectonic implications of the 3.28–3.23 Ga Fig Tree Group, central Barberton greenstone belt, South Africa. *Precambrian Research* **325**, 1–19.
Drabon N., Kirkpatrick H. M., Byerly G. R. and Wooden J. L. (2024) Trace elements in zircon record changing magmatic processes and the multi-stage build-up of Archean proto-continental crust. *Geochimica et Cosmochimica Acta* **373**, 136–150.
Frost C. D., McLaughlin J. F., Frost B. R., Fanning C. M., Swapp S. M., Kruckenberg S. C. and Gonzalez J. (2017) Hadean origins of paleoarchean continental crust in the central Wyoming province. *Bulletin of the Geological Society of America* **129**, 259–280.
Gehrels G. E., Valencia V. A. and Ruiz J. (2008) Enhanced precision, accuracy, efficiency, and spatial resolution of U-Pb ages by laser ablation-multicollector-inductively coupled plasma-mass spectrometry. *Geochemistry, Geophysics, Geosystems* **9**.
Gehrels G. and Pecha M. (2014) Detrital zircon U-Pb geochronology and Hf isotope geochemistry of Paleozoic and Triassic passive margin strata of western North America. *Geosphere* **10**, 49–65.
Gond A. K., Dey S., Zong K., Liu Y., Anand R., Mitra Anirban and Mitra Aniruddha (2023) A better understanding of Archean crustal evolution: exploring the sedimentary archive of the Singhbhum Craton, eastern India. *Journal of Asian Earth Sciences* **251**, 105630.
Griffin W. L., Belousova E. A., O'Neill C., O'Reilly S. Y., Malkovets V., Pearson N. J., Spetsius S. and Wilde S. A. (2014) The world turns over: Hadean–Archean crust–mantle evolution. *Lithos* **189**, 2–15.
Grimes C. B., Wooden J. L., Cheadle M. J. and John B. E. (2015) "Fingerprinting" tectono-magmatic provenance using trace elements in igneous zircon. *Contributions to Mineralogy and Petrology* **170**, 1–26.
Harrison T. M. (2020) *Hadean earth*., Springer Nature Switzerland AG, Cham.
Harrison T. M., Blichert-Toft J., Müller W., Albarede F., Holden P. and Mojzsis S. J. (2005) Heterogeneous hadean hafnium: Evidence of continental crust at 4.4 to 4.5 Ga. *Science* **310**, 1947–1950.
Harrison T. M., Schmitt A. K., McCulloch M. T. and Lovera O. M. (2008) Early (≥ 4.5 Ga) formation of terrestrial crust: Lu-Hf, δ18O, and Ti thermometry results for Hadean zircons. *Earth and Planetary Science Letters* **268**, 476–486.
Holden P., Lanc P., Ireland T. R., Harrison T. M., Foster J. J. and Bruce Z. (2009) Mass-spectrometric mining of Hadean zircons by automated SHRIMP multi-collector and single-collector U/Pb zircon age dating: The first 100,000 grains. *Int J Mass Spectrom* **286**, 53–63.

Hoskin P. W. O. (2005) Trace-element composition of hydrothermal zircon and the alteration of Hadean zircon from the Jack Hills, Australia. *Geochimica et Cosmochimica Acta* **69**, 637–648.
Ibañez-Mejia M., Gehrels G. E., Ruiz J., Vervoort J. D., Eddy M. E., Li C., Ibanez-Mejia M., Gehrels G. E., Ruiz J., Vervoort J. D., Eddy M. E. and Li C. (2014) Small-volume baddeleyite (ZrO2) U-Pb geochronology and Lu-Hf isotope geochemistry by LA-ICP-MS. Techniques and applications. *Chemical Geology* **384**, 149–167.
Kemp A. I. S., Wilde S. A., Hawkesworth C. J., Coath C. D., Nemchin A., Pidgeon R. T., Vervoort J. D. and DuFrane S. A. (2010) Hadean crustal evolution revisited: New constraints from Pb-Hf isotope systematics of the Jack Hills zircons. *Earth and Planetary Science Letters* **296**, 45–56.
Lenting C., Geisler T., Gerdes A., Kooijman E., Scherer E. E. and Zeh A. (2010) The behavior of the Hf isotope system in radiation-damaged zircon during experimental hydrothermal alteration. *American Mineralogist* **95**, 1343–1348.
Loucks R. R., Fiorentini M. L. and Henriquez G. J. (2020) New magmatic oxybarometer using trace elements in zircon. *Journal of Petrology* **61**.
Miller S. R., Mueller P. A., Meert J. G., Kamenov G. D., Pivarunas A. F., Sinha A. K. and Pandit M. K. (2018) Detrital zircons reveal evidence of hadean crust in the Singhbhum Craton, India. *Journal of Geology* **126**, 541–552.
Miller S. R., Mueller P. A., Meert J. G., Kamenov G. D., Pivarunas A. F., Sinha A. K. and Pandit M. K. (2019) Detrital zircons reveal evidence of hadean crust in the singhbhum craton, India: A reply. *Journal of Geology* **127**, 387–392.
Mitra Aniruddha, Dey S., Zong K., Liu Y. and Mitra Anirban (2019) Building the core of a Paleoarchean continent: Evidence from granitoids of Singhbhum Craton, eastern India. *Precambrian Research* **335**, 105436.
Mixon E. E., Bauer A. M., Blum T. B., Valley J. W., Rizo H., O'Neil J. and Kitajima K. (2024) Zircon geochemistry from early evolved terranes record coeval stagnant- and mobile-lid tectonic regimes. *Proceedings of the National Academy of Sciences* **121**, 1–8.
Mojzsis S. J., Harrison T. M. and Pidgeon R. T. (2001) Oxygen-isotope evidence from ancient zircons for liquid water at the Earth's surface 4,300 Myr ago. *Nature* **409**, 178–181.
Mukhopadhyay D. (2001) The Archaean Nucleus of Singhbhum: The Present State of Knowledge. *Gondwana Research* **4**, 307–318.
Nelson D. R., Bhattacharya H. N., Thern E. R. and Altermann W. (2014) Geochemical and ion-microprobe U-Pb zircon constraints on the Archaean evolution of Singhbhum Craton, eastern India. *Precambrian Research* **255**, 412–432.
Olierook H. K. H., Clark C., Reddy S. M., Mazumder R., Jourdan F. and Evans N. J. (2019) Evolution of the Singhbhum Craton and supracrustal provinces from age, isotopic and chemical constraints. *Earth-Science Reviews* **193**, 237–259.
Paces J. B. and Miller J. D. (1993) Precise U-Pb ages of Duluth Complex and related mafic intrusions, northeastern Minnesota: Geochronological insights to physical, petrogenetic, paleomagnetic, and tectonomagmatic processes associated with the 1.1 Ga Midcontinent Rift System. *Journal of Geophysical Research: Solid Earth* **98**, 13997–14013.
Pandey O. P., Mezger K., Ranjan S., Upadhyay D., Villa I. M., Nägler T. F. and Vollstaedt H. (2019) Genesis of the Singhbhum Craton, eastern India; implications for Archean crust-mantle evolution of the Earth. *Chemical Geology* **512**, 85–106.
Peck W. H., Valley J. W., Wilde S. A. and Graham C. M. (2001) Oxygen isotope ratios and rare earth elements in 3.3 to 4.4 Ga zircons: Ion microprobe evidence for high δ18O continental crust and oceans in the early Archean. *Geochimica et Cosmochimica Acta* **65**, 4215–4229.

Premo W. R., Castiñeiras P. and Wooden J. L. (2010) SHRIMP-RG U-Pb isotopic systematics of zircon from the Angel Lake orthogneiss, East Humboldt Range, Nevada: Is this really Archean crust? REPLY. *Geosphere* **6**, 966–972.

Ranjan S., Upadhyay D., Pruseth K. L., Nanda J. K., Lochan K. and Nanda J. K. (2020) Detrital zircon evidence for change in geodynamic regime of continental crust formation 3.7–3.6 billion years ago. *Earth and Planetary Science Letters* **538**, 116206.

Reimink J. R., Davies J. H. F. L., Bauer A. M. and Chacko T. (2020) A comparison between zircons from the Acasta Gneiss Complex and the Jack Hills region. *Earth and Planetary Science Letters* **531**, 1–10.

Rubatto D. (2017) *Zircon : The Metamorphic Mineral*., Mineralogical Society of America.

Schmitz M. D., Bowring S. A. and Ireland T. R. (2003) Evaluation of Duluth Complex anorthositic series (AS3) zircon as a U-Pb geochronological standard: New high-precision isotope dilution thermal ionization mass spectrometry results. *Geochimica et Cosmochimica Acta* **67**, 3665–3672.

Sreenivas B., Dey S., Bhaskar Rao Y. J., Vijaya Kumar T., Babu E. V. S. S. K. and Williams I. S. (2019) A new cache of Eoarchaean detrital zircons from the Singhbhum craton, eastern India and constraints on early Earth geodynamics. *Geoscience Frontiers* **10**, 1359–1370.

Sundell K., Gehrels G., Quinn D., Pecha M., Giesler D., Pepper M., George S. and White A. (2020) *AGECALCML: AN OPEN-SOURCE MATLAB-BASED DATA REDUCTION PLATFORM FOR LA-ICP-MS GEOCHRONOLOGY AND GEOCHEMISTRY DATA FROM THE ARIZONA LASERCHRON CENTER*.,

Tang M., Ji W., Chu X., Wu A. and Chen C. (2020) Reconstructing crustal thickness evolution from europium anomalies in detrital zircons. **49**, 76–80.

Trail D., Mojzsis S. J. and Harrison T. M. (2007) Thermal events documented in Hadean zircons by ion microprobe depth profiles. *Geochimica et Cosmochimica Acta* **71**, 4044–4065.

Trail D., Tailby N., Wang Y., Mark Harrison T., Boehnke P. and Harrison T. M. (2017) Aluminum in zircon as evidence for peraluminous and metaluminous melts from the Hadean to present. *Geochemistry, Geophysics, Geosystems* **18**, 1580–1593.

Trail D., Watson E. B. and Tailby N. D. (2012) Ce and Eu anomalies in zircon as proxies for the oxidation state of magmas. *Geochimica et Cosmochimica Acta* **97**, 70–87.

Trail D., Watson E. B. and Tailby N. D. (2011) The oxidation state of Hadean magmas and implications for early Earth's atmosphere. *Nature* **480**, 79–82.

Turner S., Wilde S., Wörner G., Schaefer B. and Lai Y. J. (2020) An andesitic source for Jack Hills zircon supports onset of plate tectonics in the Hadean. *Nature Communications* **11**, 1–5.

Upadhyay D., Chattopadhyay S., Kooijman E., Mezger K. and Berndt J. (2014) Magmatic and metamorphic history of Paleoarchean tonalite-trondhjemite-granodiorite (TTG) suite from the Singhbhum craton, eastern India. *Precambrian Research* **252**, 180–190.

Upadhyay D., Chattopadhyay S. and Mezger K. (2019) Formation of Paleoarchean-Mesoarchean Na-rich (TTG) and K-rich granitoid crust of the Singhbhum craton, eastern India: Constraints from major and trace element geochemistry and Sr-Nd-Hf isotope composition. *Precambrian Research* **327**, 255–272.

Watson E. B. and Harrison T. M. (2005) Zircon Thermometer Reveals Minimum Melting Conditions on Earliest Earth. *Science (1979)* **308**, 841–844.

FIGURE CAPTIONS

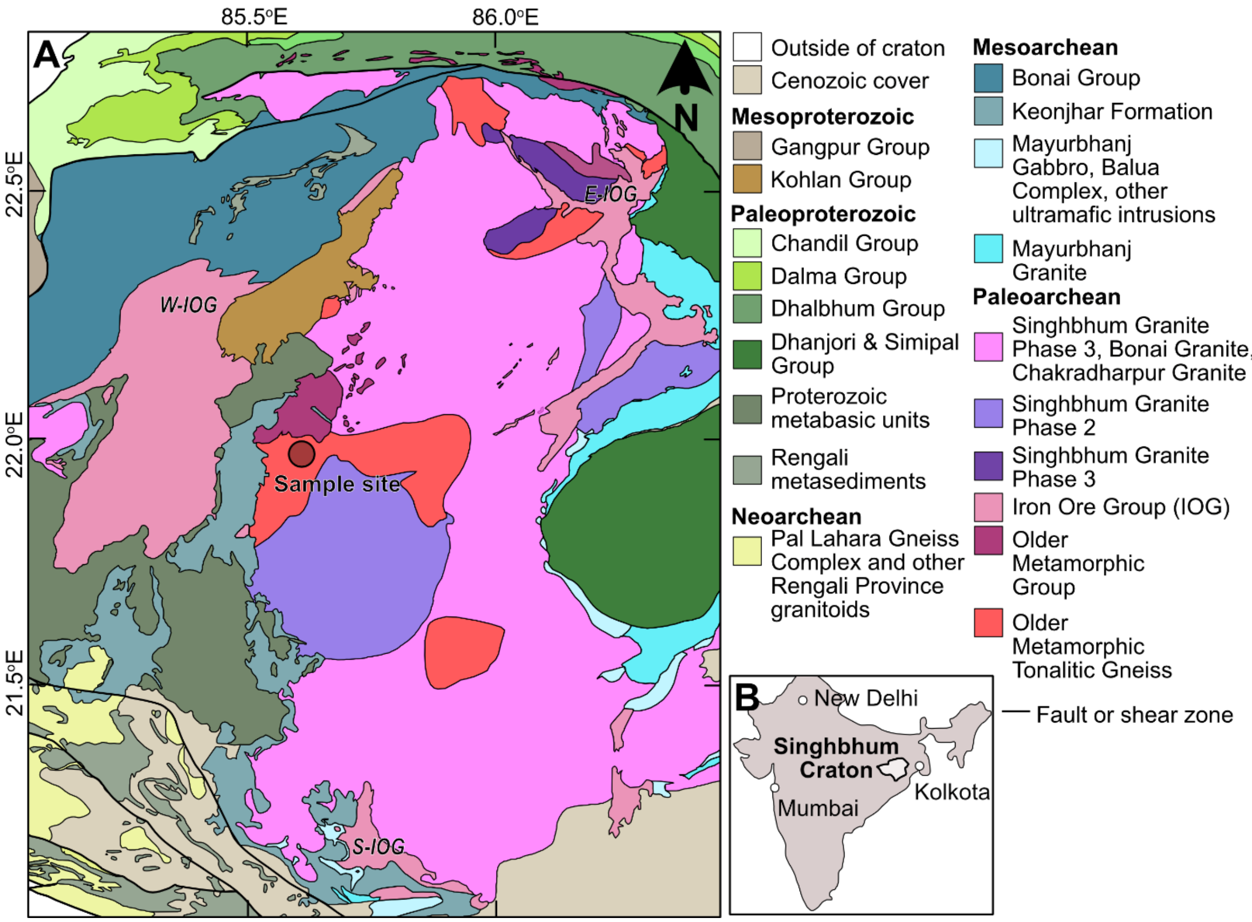

Figure 1. Part (A) shows a geologic map of a portion of the Singhbhum Craton modified after Olierook et al. (2019) and Saha (1994). Our sample site is labeled with a red dot crystal. Part (B) shows a larger map of India with the SC colored in tan.

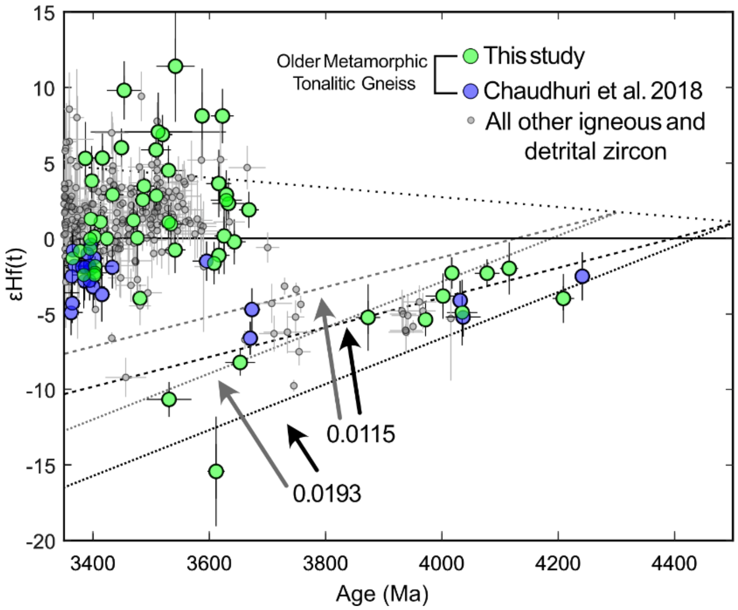

Figure 2. Time vs. ε_{HfT} for zircon 3.35 to ~ 4.2 Ga for OMTG zircons. Blue marks denote measurements by Chaudhuri et al. (2018) and green marks show points from this study. A linear regression between time and εHf returns a slope of $^{176}Lu/^{177}Hf$ = 0.010 (assuming extraction from the mantle at 4500 Ma), which is considered a mafic composition. Mantle extraction is shown for two times: (4.5 Ga- black and 4.3 Ga- gray) with each showing an evolution for a more mafic source ($^{176}Lu/^{177}Hf$ = 0.0193; dashed) and a more felsic source ($^{176}Lu/^{177}Hf$ =0.0115; dotted). Gray points denote additional S.C. igneous and detrital zircon measurements (Dey et al., 2017; Chaudhuri et al., 2018; Miller et al., 2019; Pandey et al., 2019; Sreenivas et al., 2019; Ranjan et al., 2020; Gond et al., 2023).

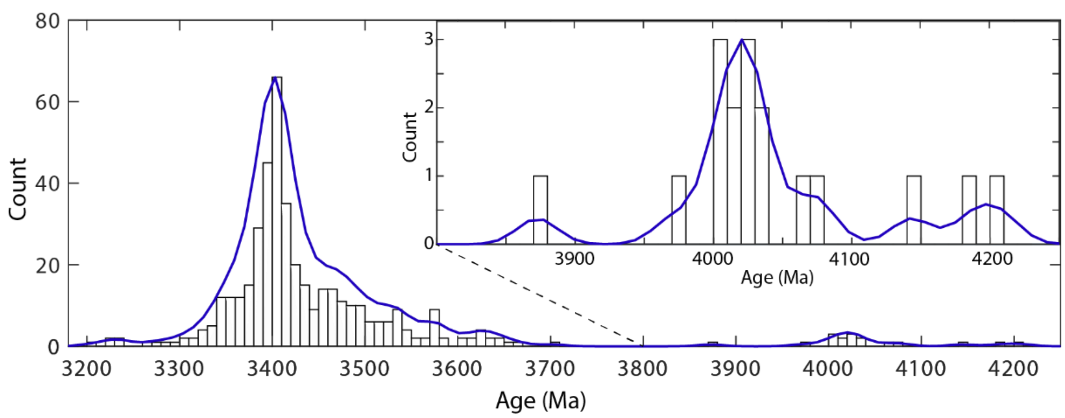

Figure 3 shows a histogram of concordant (<10% discordant) zircons from our study measured by LA-ICPMS with an inset showing ages > 3800 Ma.

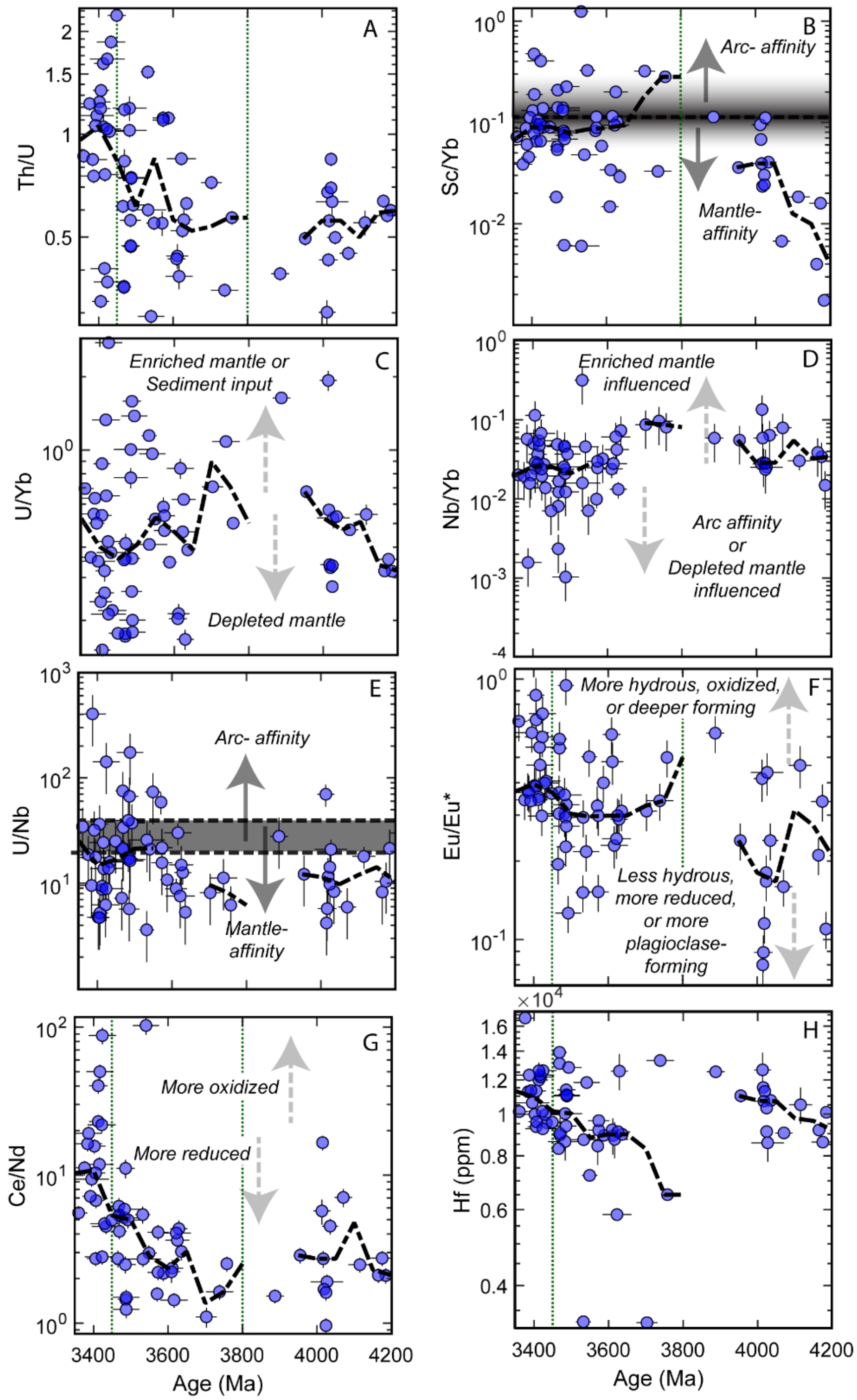

Figure 4. Time vs. a selection of trace element ratios including Th/U (A), Sc/Yb (B), U/Yb (C), Nb/Yb (D), U/Nb (E), Eu/Eu* (F), Ce/Nd (G), and [Hf] (H) for zircons > 3.35 Ga from the OMTG. Sc/Yb shows a positive correlation with time (> 3.8 Ga), potentially indicating a minority of zircons formed from fluid-present melting. We observe a large change in several trace element proxies between zircon > 3.8 Ga and < 3.8 Ga. Black lines show median values for analyses ± 50 Ma with values are calculated at 50 Ma intervals. Green, vertical, dotted lines show where means greater than and less than either 3.45 Ga or 3.8 are different at the 95% confidence level.

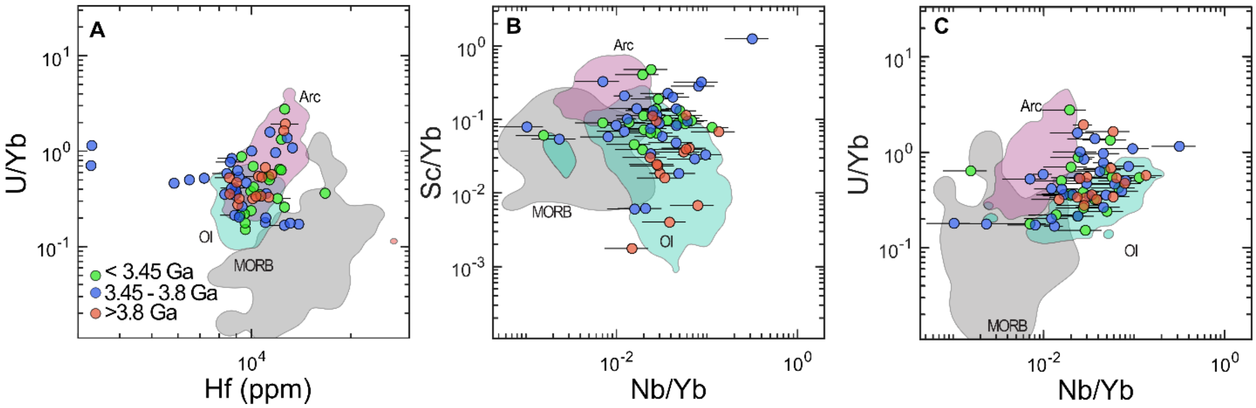

Figure 5. Compositional plots showing 90th percentile density diagrams from a compilation of ~ 4400 Phanerozoic zircon (Grimes et al., 2018; Carley et al., 2022) formed in arc (pink), mid ocean ridge (MOR; gray), and plume (ocean island; cyan) with compositions from OMTG zircon plotted (<3.45 Ga: green; 3.45-3.8 Ga: blue; >3.8 Ga: red).

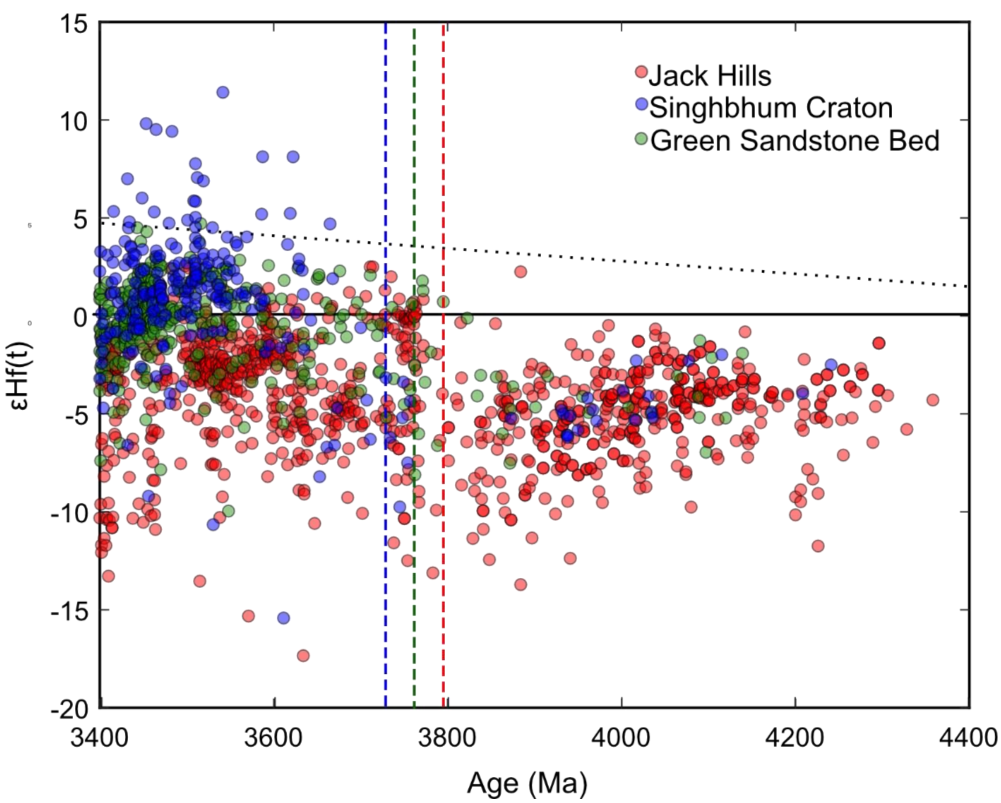

Figure 6. Time vs εH(t) for Singhbhum Craton (blue), Green Sandstone Bed (South Africa, green), and Jack Hills (Australia, blue) zircon shown. Vertical lines on part A show changes in εH(t) for each of the three sites (lines same color as points for each site). These changes are determined by changepoint analysis of 10 analysis averages for each site.

Supplemental material for “Coupled trace element and Hf-isotope measurements of Hadean through Paleoarchean zircons from the Singhbhum Craton indicate derivation from a long-lived, mantle-derived protocrust” by Heather Kirkpatrick, Emily Stoll, and Nadja Drabon

Supplementary files:

Supplemental Tables:

- Table S1: U-Pb analysis of zircon (LA-ICPMS)
- Table S2: U-Pb analysis of zircon (SHRIMP-RG)
- Table S3: In-situ zircon trace elements
- Table S4: Raw trace and rare earth element data (2023)
- Table S5: Raw trace and rare earth element data (2021)
- Table S5: Two-sample t-tests
- Table S5: Hf isotope data

Supplemental Figures:

- Figure S1: CL images of a subset of grains
- Figure S2: Time vs. concentrations of a selection of trace elements or trace element ratios
- Figure S3: Time vs. concentrations of a selection of trace element concentrations which assess sedimentary input
- Figure S4: εHf(t) vs. age for OMTG zircon grouped by zoning or trace element status
- Figure S5: Time vs. several trace element concentrations, proxies, or ratios for the Jack Hills (Australia), Green Sandstone Bed (South Africa), and Older Metamorphic Tonalitic Gneiss (India).

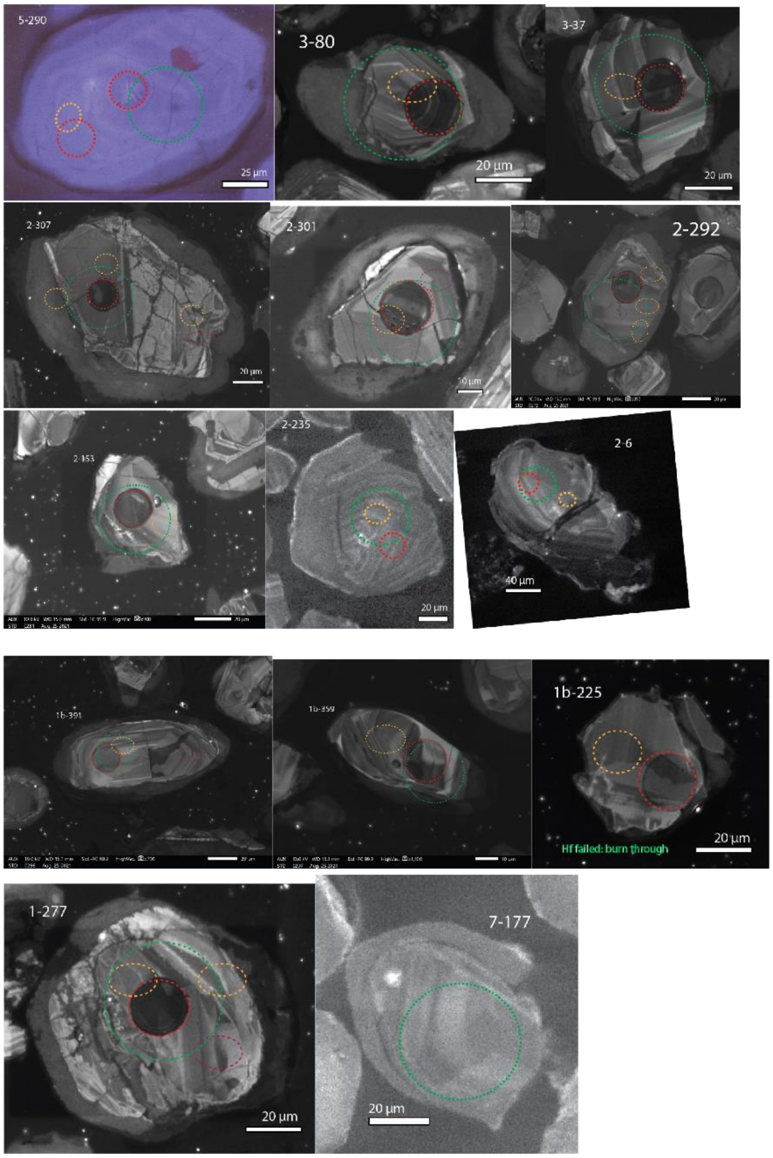

Figure S1: CL images of a subset of grains. Green, red, yellow-orange, and dark pink spots denote Hf analysis, LA-ICPMS U-Pb analysis, SHRIMP TREE analysis, and SHRIMP U-Pb analysis, respectively.

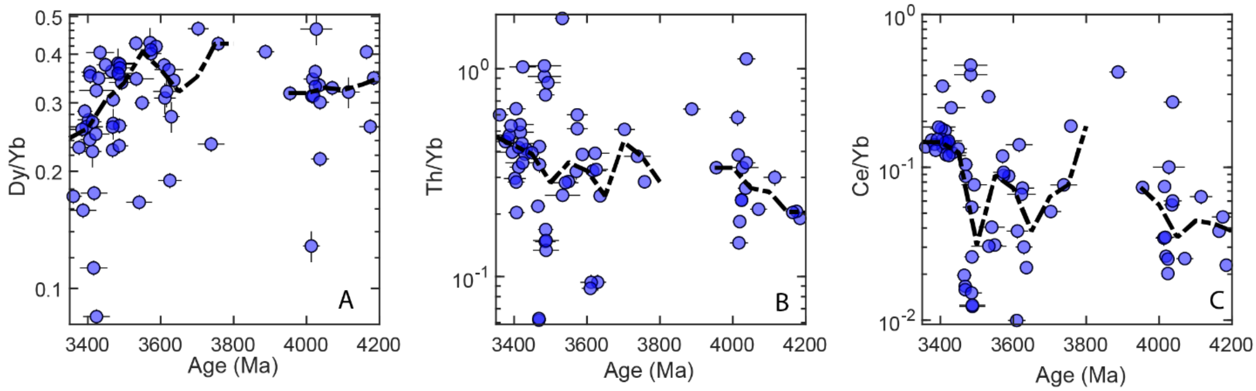

Figure S2: Time vs. concentrations of a selection of trace elements or trace element ratios including Dy/Yb (A), Th/Yb (B), and Ce/Yb (ppm) (C) for zircons >3.35 Ga from the OMTG. Black lines show median values for analyses ± 50 Ma with values calculated at 50 Ma intervals.

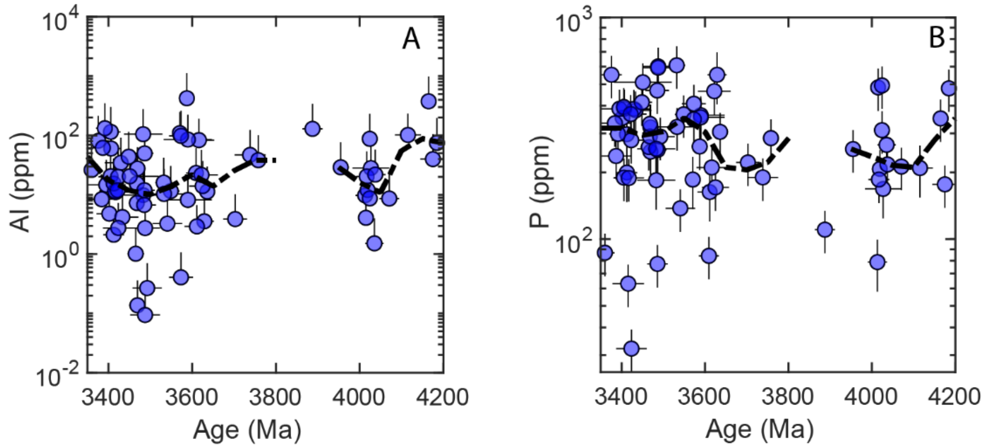

Figure S3: Time vs. concentrations of a selection of trace element concentrations which assess sedimentary input including [A] Al (ppm) (Trail et al., 2017) and [B] P (ppm) (Burnham and Berry, 2017) for zircons >3.35 Ga from the OMTG. Black lines show median values for analyses ± 50 Ma with values calculated at 50 Ma intervals.

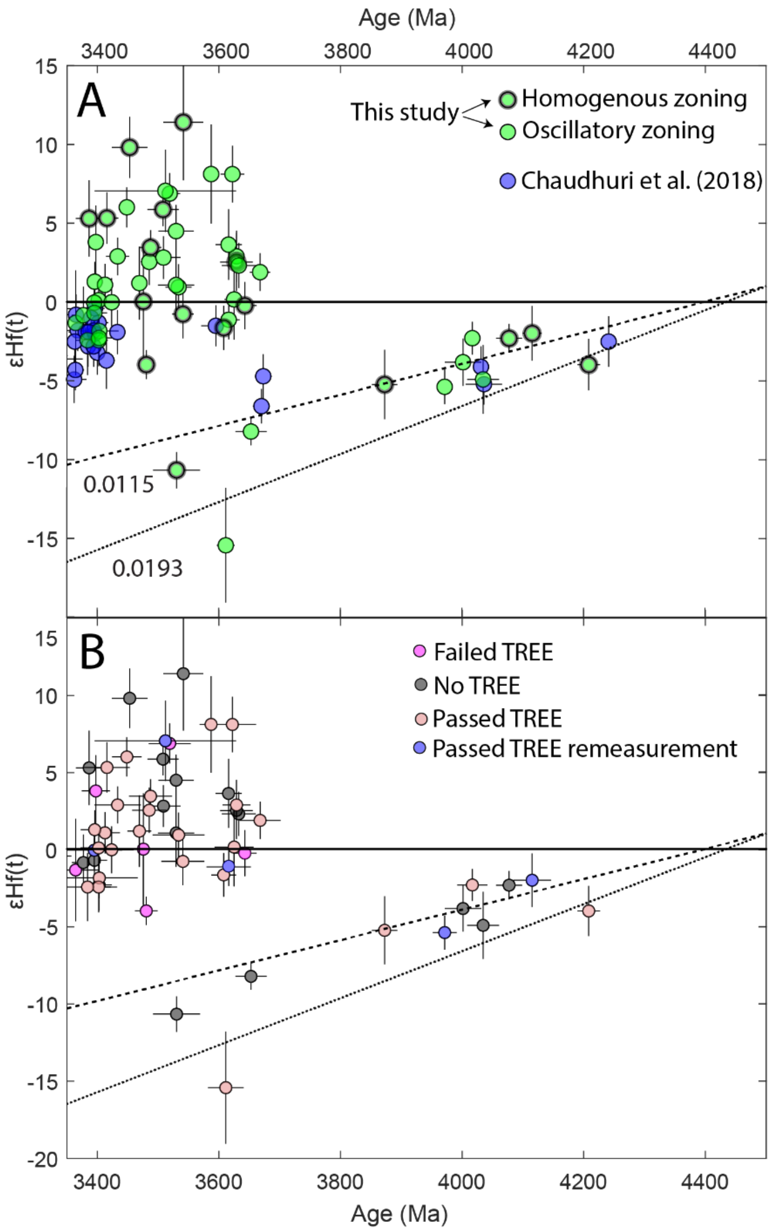

Figure S4: εHf(t) vs. age for OMTG zircon grouped by zoning or trace element status. Part A shows points from this study (green) identified by zoning type (oscillatory (thin outline) vs. homogenous zoning (thick outline)) and points published in Chaudhuri et al. (2018) (blue). Part B shows analyses from this study grouped by whether they failed (pink), passed on remeasurement (blue), or passed (salmon) our TREE filters. Alternatively, grey shows points where TREE measurements were not performed.

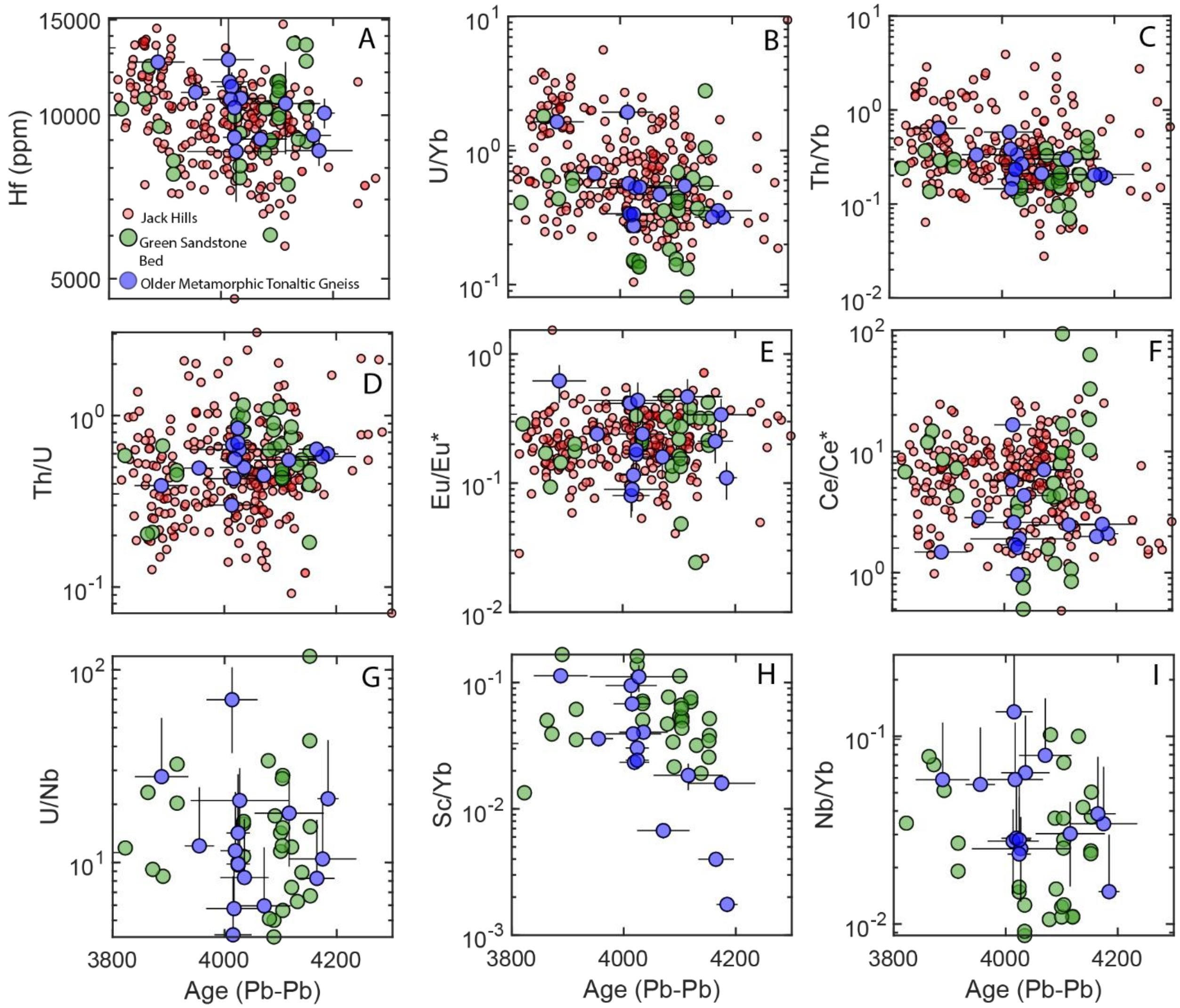

Figure S5: Time vs. several trace element concentrations, proxies, or ratios for the Jack Hills (Australia; red), Green Sandstone Bed (South Africa; green), and Older Metamorphic Tonalitic Gneiss (India, blue), including [A] Hf concentration; [B] U/Yb; [C] Th/Yb; [D] Th/U; [E] Eu/Eu*; [F] Ce/Ce*; [G] U/Nb; [H] Sc/Yb; and [I] Nb/Yb. Error bars (2 s.d.) are shown only for Older Metamorphic Tonalitic Gneiss data.

References

Burnham, A.D., and Berry, A.J., 2017, Formation of Hadean granites by melting of igneous crust: Nature Geoscience, v. 10, p. 457–461, doi:10.1038/ngeo2942.

Chaudhuri, T., Wan, Y., Mazumder, R., Ma, M., and Liu, D., 2018, Evidence of Enriched, Hadean Mantle Reservoir from 4.2-4.0 Ga zircon xenocrysts from Paleoarchean TTGs of the Singhbhum Craton, Eastern India: Scientific Reports, v. 8, p. 1–12, doi:10.1038/s41598-018-25494-6.

Trail, D., Tailby, N., Wang, Y., Mark Harrison, T., Boehnke, P., and Harrison, T.M., 2017, Aluminum in zircon as evidence for peraluminous and metaluminous melts from the Hadean to present: Geochemistry, Geophysics, Geosystems, v. 18, p. 1580–1593, doi:10.1002/2016GC006794.